Toxicology and Applied Pharmacology 338 (2018) 197–203

Contents lists available at ScienceDirect

Toxicology and Applied Pharmacology

journal homepage: www.elsevier.com/locate/taap

Fullerene (C60) particle size implications in neurotoxicity following infusion into the hippocampi of Wistar rats

Ândrea Barbosa Kraemer, Gustavo Morrone Parfitt, Daiane da Silva Acosta, Gisele Eva Bruch, Marcos Freitas Cordeiro, Luis Fernando Marins, Juliane Ventura-Lima, José Maria Monserrat, Daniela Martí Barros*

Programa de Pós-Graduação em Ciências Fisiológicas, Universidade Federal do Rio Grande - FURG, Rio Grande, RS, Brazil

ARTICLE INFO

Keywords:
Buckminsterfullerene
Hippocampus
Learning
Memory
Nanotechnology

ABSTRACT

The buckminsterfullerene (C60) is considered as a relevant candidate for drug and gene delivery to the brain, once it has the ability to cross the blood-brain barrier. However, the biological implications of this nanomaterial are not fully understood, and its safety for intracerebral delivery is still debatable. In this study, we investigated if C60 particle size could alter its biological effects. For this, two aqueous C60 suspensions were used with maximum particle size up to 200 nm and 450 nm. The suspensions were injected in the hippocampus, the main brain structure involved in memory processing and spatial localization. In order to assess spatial learning, male Wistar rats were tested in Morris water maze, and the hippocampal BDNF protein levels and gene expression were analyzed. Animals treated with C60 up to 450 nm demonstrated impaired spatial memory with a significant decrease in BDNF protein levels and gene expression. However, an enhanced antioxidant capacity was observed in both C60 treatments. A decrease in reactive oxygen species levels was observed in the treatments with suspensions containing particles measuring with up to 450 nm. Thiobarbituric acid reactive substances, glutamate cysteine ligase, and glutathione levels showed no alterations among the different treatments. In conclusion, different particle sizes of the same nanomaterial can lead to different behavioral outcomes and biochemical parameters in brain tissue.

1. Introduction

Carbon nanomaterials (NMs) are formed by carbon molecules arranged in hexagonal (sometimes pentagonal and heptagonal) rings, ultimately forming cylinders (buckytubes) or spheres (buckyballs). The buckminsterfullerene (C60) is a buckyball consisting of 60 carbon molecules arranged in a truncated icosahedron of 20 hexagons and 12 pentagons of approximately 1 nm diameter each, resulting in a quasi-spherical cage-like structure (Bhattacharya et al., 2016; Kroto et al., 1985). C60 are considered as relevant candidates for drug and gene delivery (Chen et al., 2015; Dellinger et al., 2013; Maeda-Mamiya et al., 2010), being one of the types of manufactured NMs with the ability to cross the blood-brain barrier (Hsieh et al., 2017).

The blood-brain barrier (BBB) is one of the main obstacles for the pharmacological treatment of central nervous system disorders. Only molecules with very low molecular mass and high lipophilicity are able to cross the BBB and reach inner brain structures, limiting the therapeutic alternatives (Hersh et al., 2016). In the last years, many different types of NMs have been developed and tested as nanocarriers, aiming to help therapeutic molecules to cross the BBB (Khalin et al., 2014).

If on the one hand C60 are promising for their facilitated uptake, this same characteristic can raise some concerns. Indeed, previous reports have shown that C60 can exert toxicity via inflammatory responses, decrease in energetic metabolism, oxidative stress, growth inhibition, and behavioral impairments (Brausch et al., 2011; Johnston et al., 2010; Larner et al., 2017; Usenko et al., 2008; Zhu et al., 2008). It is known that NMs can be endocytosed into cells, reaching neurobiologically relevant structures, and may change the normal function of these cells (Oberdörster, 2004). However, information concerning the effects of C60 exposure in terms of spatial memory and biochemical responses is still scarce. There are a few studies testing fullerenes and its derivatives, and this is an important issue to consider since different types of functionalization can give rise different biological effects (Lin et al., 1999; Yamada et al., 2010). Furthermore, the physiochemical properties, impact on reactive oxygen species (ROS), and toxicity of a

* Corresponding author at: Laboratório de Neurociências, Instituto de Ciências Biológicas (ICB), Universidade Federal do Rio Grande – FURG, Cx. P. 474, CEP 96203-900 Rio Grande, RS, Brazil.
E-mail address: barrosdm@yahoo.com.br (D.M. Barros).

https://doi.org/10.1016/j.taap.2017.11.022
Received 25 August 2017; Received in revised form 23 November 2017; Accepted 26 November 2017
Available online 27 November 2017
0041-008X/

nanomaterial can lead to different results even in its pristine form, depending on the manufacturing techniques (Markovic and Trajkovic, 2008).

The hippocampus plays a pivotal role in spatial learning and memory, being this process dependent on brain-derived neurotrophic factor (BDNF) activation (Gil-Bea et al., 2011; Pilly and Grossberg, 2012). BDNF is synthesized, stored and secreted from the dendrites of excitatory neurons, mainly during basal neurogenesis and adult hippocampal neurogenesis (Kim et al., 2011). Environmental contaminants, drugs, and lesions may affect hippocampal function by decreasing BDNF levels, resulting in learning impairments (Bavithra et al., 2015; Gil-Bea et al., 2011).

Considering the ability of C60 to reach the brain tissue, it is important to investigate if the exposure to this NM can lead to neurotoxic effects. Thus, the objective of this study was to evaluate if the intracerebral administration of C60 suspensions with different particle sizes can induce oxidative stress, alter BDNF levels, and affect spatial memory.

2. Material and methods

2.1. Preparation of the fullerene suspension

An aqueous C60 suspension (200 mg/L; SES Research, 99% purity) was stirred in MilliQ water for two months under constant artificial white light. After stirring, the suspension was centrifuged for one hour at 15 °C at 25000 × *g*, and then filtered sequentially through 450 nm and 200 nm filters. Next, suspensions were characterized using atomic force microscopy (AFM).

2.2. Animal models

Fifty Wistar rats (male, 2–3 months of age, weighing 250–280 g) were obtained from a breeding colony at the Federal University of Rio Grande (Brazil). The animals were maintained in groups of five per cage under a 12-h light/dark cycle and at a temperature of 22 °C ± 1 °C, with food and water provided ad libitum. All of the animal procedures were performed in accordance with the Animal Care and Use Committee of the Brazilian College of Animal Experiments (COBEA - Brazil), and all efforts were made to reduce the number of animals used and to limit their suffering.

2.3. Stereotactic surgery

Animals were deeply anesthetized with ketamine (62.5 mg/kg) and xylazine (13 mg/kg) and placed in the stereotactic apparatus. The scalp was cut open and two holes were drilled in the skull (starting from bregma, anteroposterior 4.3 mm, centrolateral 3.0 mm, dorsoventral 1.8 mm) (Paxinos and Watson, 2007), so that the guide cannulae could be implanted right above the dorsal CA1 region of both hippocampi. Cannulae were fixed to the skull with an autopolymerizing dental acrylic resin (Barros et al., 2004). Total recovery time was of 48 h.

2.4. Behavioral task

In order to assess possible alterations in spatial learning, animals were subjected to a modified version of the Morris water maze (MWM) (Morris, 1984). The MWM apparatus consisted of a circular dark tank (168 cm diameter) filled with black-dyed water (70 cm deep, 24 ± 1 °C) divided into four imaginary quadrants. The room also had visual cues fixed in the walls. Animals were trained for five days and tested on the sixth day. During the training sessions, a platform was placed in one of the four virtual quadrants, with its top hidden just below the water surface. Each training session consisted of four trials, separated by 70 s intervals. Animals were placed in a different quadrant for each trial, and had up to 120 s to find the hidden platform. Learning progress was evaluated by the time taken to reach the hidden platform (escape latency). In the test day, the platform was removed and the animals were tracked for 90 s. Learning retention was estimated by the time spent in the quadrant where the platform originally was. Data was obtained and analyzed using a video tracking system (EthoVision®, NOLDUS).

2.5. Intracerebral infusions

Saline or C60 suspensions (1 μL) were slowly administered immediately after each training session. NT suspensions contained C60 measuring either ≤ 200 nm or ≤ 450 nm (experimental groups C60 ≤ 200 and C60 ≤ 450, respectively). For the intrahippocampal injections, 27-gauge infusion cannulae were manually inserted into the guide cannulae that were fixed in the skull in the stereotactic surgery. To successfully reach the hippocampi, the infusion cannulae were 1 mm longer than the guide cannulae.

2.6. Biochemical and molecular analysis

2.6.1. Real time quantitative PCR to assess BDNF gene expression

After MWM test session, rats were decapitated and the brains were immediately removed for the isolation and storage of the hippocampi at − 80 °C. Samples were homogenized in TRIzol (Invitrogen) for total RNA extraction. For complementary DNA (cDNA) synthesis, KIT High Capacity cDNA Reverse Transcription (Applied Biosystems) was utilized. cDNA samples were used to analyze the expression of the target gene BDNF using the RT-qPCR technique. We used the following specific primers for BDNF: ((F) 5′-GGCCCAACGAAGAAAACCAT-3′; (R) 5′-AGCATCACCCGGGAAGTG-3′), normalized against GAPDH: ((F) 5′-TGCACCACCAACTGCTTA-3′; (R) 5′-GGATGCAGGGATGATGTTC-3′). Sequences were based on the ones available in the worldwide gene bank (GenBank: http://www.ncbi.nlm.nih.gov). RT-qPCR was performed using the SYBR Green system on a PCR 7500 (Applied Biosystems) device according to the following protocol: denaturation at 95 °C for 10 min, amplification at 95 °C for 15 s, and 60 °C for 1 min, for 45 cycles. The resulting curves were analyzed at the end of the PCR to confirm the identity of the products.

2.6.2. ELISA method to detect BDNF levels

Isolated hippocampi were homogenized in lysis buffer, centrifuged, and the supernatant was collected. The sample was diluted by adding 4 equivalents of Dulbecco's Phosphate Buffered Saline solution (DPBS), and the protocol was performed according to the instructions provided by the manufacturer (PROMEGA BDNF E_{max}® ImmunoAssay Systems).

2.6.3. Measurement of reactive oxygen species

Brain samples were homogenized immediately after isolation (1:5 *w/v*) in ice-cold buffer (40 mM Tris-HCl- pH 7.4). After centrifugation, supernatants were used to determine ROS levels using 2′, 7′-dichlorofluorescein-diacetate (H_2DCF-DA, Sigma-Aldrich, USA), generating fluorochromes that could be detected using excitation/emission wavelengths of 488 nm and 525 nm, respectively. Readings were performed using a fluorescence microplate reader (Perkin Elmer Victor 2 fluorescence, USA).

2.6.4. Lipid peroxide content

Lipid peroxidation was quantified using the thiobarbituric acid reactive substances (TBARS) method (Oakes and Van Der Kraak, 2003). The fluorescence was measured at wavelengths of 515 nm and 553 nm for excitation and emission, respectively. Oxidative damage to lipids was expressed as nmols of equivalents of TMP (1,1,3,3-tetramethoxypropane as standard reaction) per mg of tissue, based on the TMP curve.

2.6.5. Determination of the reduced glutathione (GSH) concentration and glutamate cysteine ligase (GCL) activity

Glutamate cysteine ligase (GCL) activity and baseline glutathione determination were estimated based on the reaction of naphthalene dicarboxaldehyde (NDA) with glutathione (GSH) or γ-glutamylcysteine (γ-GC) to form cyclized highly fluorescent products (White et al., 2003). NDA-GSH fluorescence intensity was measured (472 ex/528 em) using a fluorescence microplate reader (Victor 2, Perkin Elmer). This assay demonstrates an advantage that baseline levels of GSH can also be measured in the same tissue sample. For GCL activity, a GCL reaction cocktail was prepared (400 mM Tris-HCl, 40 mM ATP, 20 mM glutamate, 2.0 mM EDTA, 20 mM sodium borate, 2 mM serine, and 40 mM MgCl) immediately before the start of the assay to prevent ATP degradation. Samples were maintained on ice until they were transferred to the reaction plate (25 °C) at 15 s intervals. After 5 min of pre-incubation, the GCL reaction was initiated by adding 50 μL of cysteine (2 mM) to each GCL activity well (cysteine was not added to the GSH-baseline wells at this time). The plate was then incubated for 30 min, and the reaction was stopped by adding 50 μL of 5-sulfosalicylic acid (SSA, 200 mM). Next, 50 μL of 2 mM cysteine was added to the GSH-baseline wells. After protein precipitation, the plate was centrifuged for 5 min at 2000 × *g* and 20 μL aliquots of the supernatant from each well of the reaction plate were transferred into a 96-well plate for fluorescence detection (Victor 2, Perkin Elmer).

2.6.6. Determination of the antioxidant capacity against peroxyl radicals

The antioxidant capacity against peroxyl radicals was measured based on the ROS production in the homogenate treated with or without the peroxyl radical generator (Amado et al., 2009). The peroxyl radicals were produced through the thermal decomposition (35 °C) of ABAP 2,2′-azobis (2 methylpropionamidine) dihydrochloride (Winston et al., 1998). Immediately before the reading on the fluorescence microplate reader (Victor 2, Perkin Elmer), 10 μL of the fluorescent probe 2′,7′ dichlorofluorescein diacetate (H_2DCF-DA) was added to each well at a final concentration of 40 μM H_2DCF-DA (Ferreira-Cravo et al., 2007), followed by cleavage by esterases that are present in the samples. In addition, the non-fluorescent compound H_2DCF, which is oxidized by ROS into the fluorescent compound DCF, was detected at wavelengths of 488 and 525 nm for excitation and emission, respectively. The generation of the total fluorescence was calculated by integrating the fluorescence unit (FU) against time, adjusting the FU data to a second-order polynomial function. The relative difference between the ROS area with or without ABAP was considered as a measure of antioxidant capacity, with the high area representing the minor antioxidant capacity because high fluorescence levels were obtained after the addition of ABAP, indicating a low antioxidant capacity against peroxyl radicals.

Total protein content was analyzed using a commercial kit (Doles Ltd., Brazil) based on the Biuret method. The determinations of the protein and enzyme levels were performed at least in triplicate.

2.7. Statistical analysis

After confirming assumptions of normality and homoscedasticity, significant differences between groups were tested using analysis of variance (ANOVA), followed by the Newman-Keuls post-test. All data is represented as mean ± SEM, and differences were considered as statistically significant at $p < 0.05$.

3. Results

Images of filtered aqueous suspensions of C60 deposited on a mica substrate were obtained using an atomic force microscope (AFM). Dots with nanometer sizes indicated the presence of C60 nanoparticles. Aggregates of C60 demonstrated a maximum height of 6.7 nm with a mean height of 4.4 nm after filtration using a 200 nm pore filter (Fig. 1A). In contrast, after filtration with the 450 nm pore filter, the C60 aggregates displayed a maximum height of 70 nm, with a mean height of 15.3 nm (Fig. 1B). This finding was consistent with previously published results (Andrievsky et al., 2002).

In the second day of the training phase of the MWM, animals from all groups showed reduced escape latency, suggesting no impairments in memory and learning in this time period. However, animals from the C60 ≤ 450 group showed more difficulty to learn the task in the long term, with the worst performance in the last day of training (Fig. 2A). Accordingly, the C60 ≤ 450 group spent less time in the target quadrant during the test session ($p < 0.05$) (Fig. 2B).

After the behavioral tests, we evaluated the hippocampal BDNF gene expression and protein levels. BDNF gene expression was reduced in the C60 ≤ 450 group when compared to control ($p < 0.05$) (Fig. 3A). Furthermore, in this same group the BDNF protein levels were significantly diminished ($p < 0.05$) in comparison to the other groups (Fig. 3B).

ROS concentration was analyzed immediately after tissue removal, and we found a significant decrease in ROS concentration ($p < 0.05$) in the C60 ≤ 450 group (Fig. 4A). However, no significant changes in the TBARS content were observed among the treatments ($p < 0.05$) (Fig. 4B).

Concerning the impacts in the antioxidant defenses, the GCL activity and GSH levels were not affected by C60 treatment ($p < 0.05$) (Fig. 5A and B, respectively). The hippocampal antioxidant capacity against peroxyl radicals showed an increase in both treated groups when compared to the control group ($p < 0.05$) (Fig. 5C).

4. Discussion

It is known that NMs can be endocytosed into cells, reaching neurobiologically relevant structures, and may change the normal function of these cells (Oberdörster, 2004). However, information concerning the effects of C60 exposure in terms of spatial memory and biochemical responses is still scarce.

The potential effect of different sizes of C60 on spatial memory was assessed through the MWM task. From the third day on, animals exposed to ≤450 nm C60 started showing impairments in spatial memory, suggesting that C60 suspensions with larger particle sizes can affect the consolidation of spatial memory. The consolidation of memory requires the involvement of several factors, including BDNF. BDNF is broadly expressed in the mammalian brain, and is involved in many neurological processes, including antidepressant effects, mood changes, anxiety disorders, and synaptic plasticity, which is directly involved in long-term memory (Bekinschtein et al., 2007). In this study, we observed a significant decrease in BDNF mRNA and protein levels in the hippocampus of animals treated with C60 dispersions with larger particles. These animals also showed impairments in learning and spatial memory. Several studies have shown an association between BDNF levels with learning and memory, including spatial memory (Francis et al., 2012; Petzold et al., 2015; Radiske et al., 2017). Patients with Alzheimer's disease show low expression of BDNF (Connor and Dragunow, 1998), and this may be in part responsible for the memory loss. Additionally, previous studies have suggested that stress downregulates BDNF (Pisu et al., 2011), and a prolonged period of exposure to several compounds, including NMs, can be considered as stress.

An important mechanism attributed to NM exposure is the generation of ROS and oxidative stress (Oberdörster, 2004; Wang et al., 2014). Sayes et al. (2004) have demonstrated that fullerene generates superoxide anion radicals and damages cell membranes, thereby inducing cellular death. Fullerenes are redox-active compounds, which can affect lipid-rich tissues such as the brain, which additionally has a low antioxidant capacity when compared to other organs. In fact, lipid peroxidation was also observed in fish exposed to C60 (Ferreira et al., 2012; Oberdörster, 2004). It is known that C60 is a photosensitizer, which induces the production of ROS in the presence of light (Goodarzi et al.,

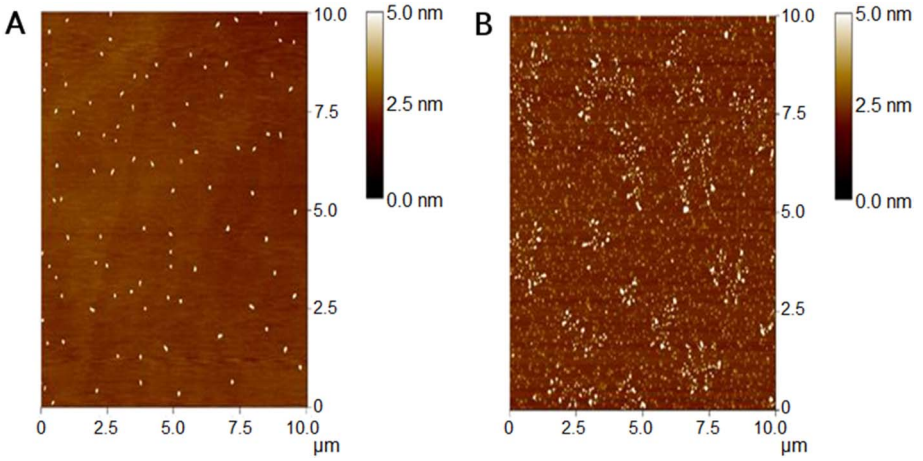

Fig. 1. Atomic force microscopy imaging of C60 suspensions with particles measuring ≤ 200 nm (A) or ≤ 450 nm (B).

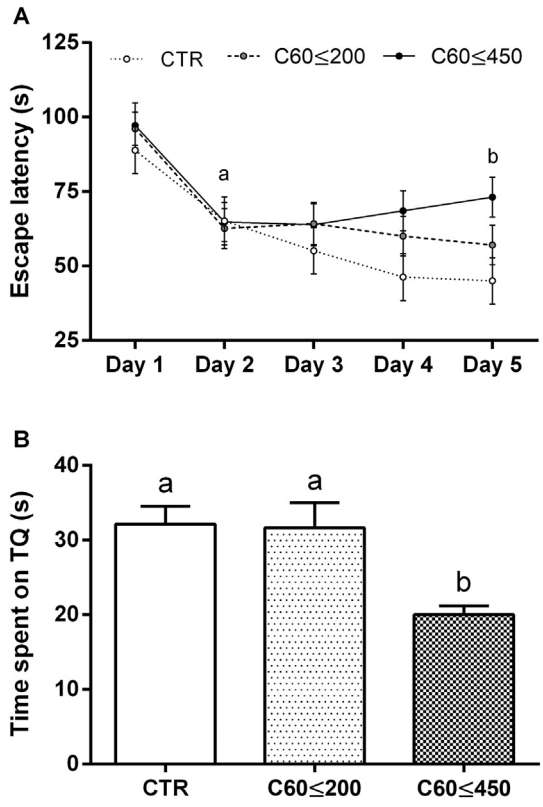

Fig. 2. Effects of the intrahippocampal infusions of C60 on spatial memory, assessed through the Morris water maze test. C60 was administered immediately after each training session, in suspensions with particles measuring ≤ 200 nm or ≤ 450 nm (groups C60 ≤ 200 and C60 ≤ 450, respectively). Animals from all groups performed better in the second day of training (a = $p < 0.05$, day 1 vs. day 2, all groups), but on the last day animals from the C60 ≤ 450 group showed a longer escape latency time ([F (2, 50) = 5.899], b = $p < 0.01$, C60 ≤ 450 vs. control) (A). Accordingly, animals treated with the suspension with larger particles (C60 ≤ 450) spent less time in the target quadrant (TQ) during the test session, indicating more difficulty to learn the task (different letters indicate statistically significant differences between groups [F (2, 17) = 7.6523, $p < 0.05$)] (B).

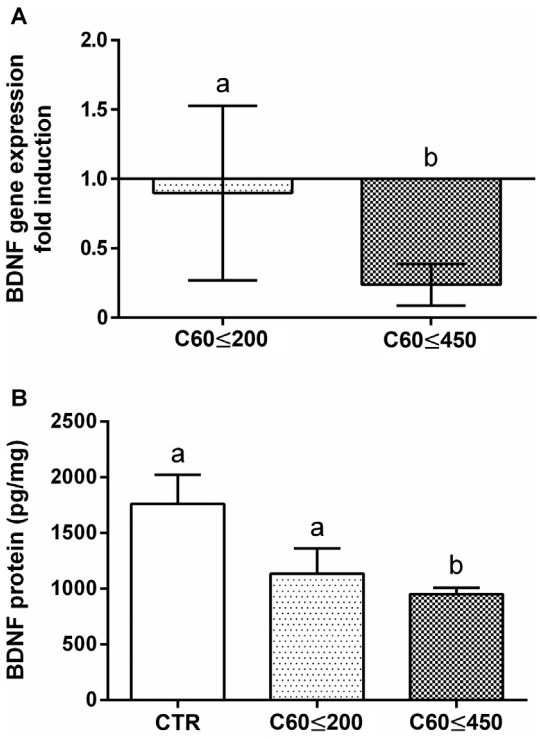

Fig. 3. Alterations in BDNF gene expression and protein levels in the rat hippocampus following the intra-structure administration of C60 suspensions with different particle sizes. Infusion of C60 suspensions particles measuring up to 450 nm (group C60 ≤ 450) significantly reduced both BDNF gene expression (A) and protein levels (B) in the hippocampus [F (2, 11) = 4.5262 and F (2, 11) = 4.4542, respectively]. Different letters indicate significant differences ($p < 0.05$) between the different groups (n = 4–5 per group).

2017; Hotze et al., 2008). Thus, the pro-oxidant function attributed to C60 is mostly related to visible light and/or UV due to the promotion of the long-live tripled excitation and posterior energy transfer to oxygen, which generates ROS that can damage macromolecules such as lipids, proteins, and nucleic acids (Markovic and Trajkovic, 2008).

We observed a reduction in ROS concentration after exposure to ≤ 450 nm C60 dispersions. Several studies have attributed C60 antioxidant activity to its high free radical scavenger ability (Markovic and Trajkovic, 2008). It was already observed that C60 exerted antioxidant effects in different mammal cells (Ehrich et al., 2011; Kato et al., 2010; Xiao et al., 2005). On the one hand, ROS reduction suggests less brain damage, but animals treated with ≤ 450 nm C60 showed impairment in learning and spatial memory. Reduction in BDNF levels offer one explanation for this, but H_2O_2 is also known to play an important role as a second messenger in synaptic plasticity (Kato et al., 2010). It can be hypothesized that C60 reducing H_2O_2 levels by its radical scavenging activity, impairing signaling pathways associated with learning and memory. However, additional studies are required to confirm this hypothesis.

Lipid damage was observed in this study, which was most likely due to the C60 exposure in the dark. C60 is photo-excitable, and possesses a

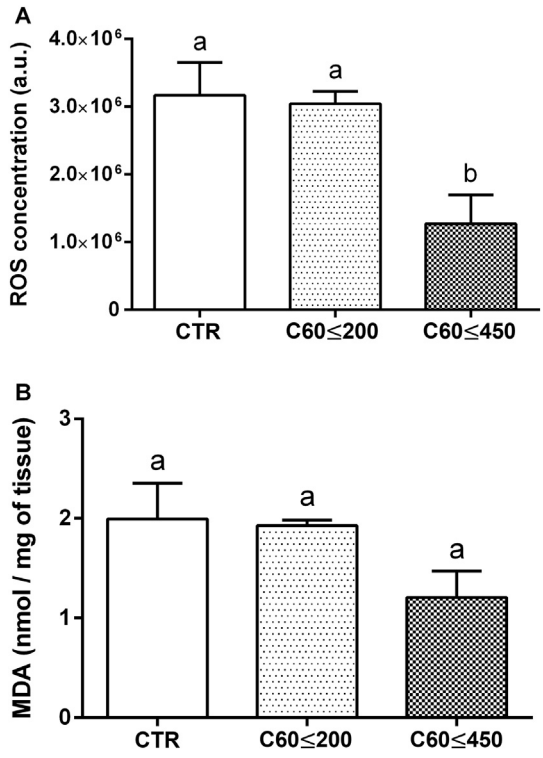

Fig. 4. Hippocampal concentration of reactive oxygen species (ROS) and malondialdehyde (MDA) following treatment with C60 suspensions with different particle sizes. The hippocampus of animals treated with the suspension containing C60 measuring up to 450 nm (group C60 ≤ 450) showed a smaller concentration of ROS [$F(2, 10) = 8.8646$, $p < 0.05$] (A). However, no significant differences were observer between groups in MDA content [$F(2, 10) = 3.8313$] (B). Different letters indicate significant differences ($p < 0.05$) between treatments (n = 3–5 per group).

high capacity to react with oxygen forming ROS, which can damage biological molecules (Ferreira et al., 2012). In rat liver microsomes, C60 exposure in the presence of UV or fluorescent light resulted in an increase in lipid peroxidation and proteins damage (Kamat et al., 1998).

GCL is the limiting step in GSH synthesis (White et al., 2003). GCL activity may be modulated in response to an alteration of the cellular redox-state. Zebrafish embryos showed an increase in GCL gene expression and glutathione-S-transferase (GST) following exposure to C60. It is possible that fullerene acts as a radical-sponge, not providing sufficient ROS to alter the redox-state of the hippocampus, even with the observed modulation in GCL activity. It is known that ROS can interact with the sulfhydryl groups of the Keap1 protein, which binds to the NRf2 factor and liberates the protein, enabling its translocation into the nucleus. Subsequently, this initiates the expression of genes involved in antioxidant capacity and consequently enhances protein levels (Pi et al., 2008).

In our study, we could not detect alterations in GCL activity and GSH levels, indicating that C60 exposure did not alter the redox-state in the hippocampus. However, other studies have shown that fullerene can have an effect in the levels of GSH. For example, exposure to C60 were reported to induce a decrease in GSH levels in the brains of *Carassius auratus* (Zhu et al., 2008), while GSH levels were enhanced in *Fundulus heteroclitus* after exposure to C60 aggregates (Blickley and McClellan-Green, 2008). These results indicate that C60 can act in the GSH system in different forms, dependent on variables such as the animal model and the exposure conditions.

C60 appeared to induce alterations in the antioxidant capacity. In a previous report, the lungs of rats treated with functional C60 revealed the modulation of the antioxidant system via an increase in glutathione-peroxidase (GPx) and superoxide dismutase (SOD) activities. Concomitantly, there was also an increase in the GSH levels and a decrease in the glutathione oxidized (GSSG) and lipid peroxidation levels (Injac et al., 2009). In our study, an increase in the total antioxidant capacity against peroxyl radicals was observed in animals treated with both C60 particle sizes when compared to the control group. This result suggested that exposure to C60 modulated the antioxidant capacity in the hippocampus independent of particle size.

The C60 aqueous suspensions used in this work contained fullerenes of two different maximum particle sizes, obtained through sequential filtration. Particle sizes were assessed through AFM, which is a suitable approach for suspensions containing particles with different sizes (Hoo et al., 2008). However, the number of fullerenes successfully delivered in each intrahippocampal injection could not be determined, being this a limitation of our study.

5. Conclusions

C60 exposure impaired learning and spatial memory, as shown by the alterations observed in the behavioral tasks and the decrease in BDNF levels. In oxidative stress, larger C60 particles (≤ 450 nm) exert an antioxidant role after a decrease in ROS concentration; however, no lipid damage or increases in the total antioxidant capacity were observed. Thus, in this study, C60 exposure resulted in two different outcomes: first, the diminishment of learning and spatial memory, and second, the concomitant decrease in BDNF levels and other antioxidant activities. On the basis of these results, nanoparticles with a high antioxidant capacity may diminish cognitive capacity in learning and spatial memory. Thus, the overall conclusions derived from the fullerene treatments, including the titration of larger particles, might provide further insight towards therapies to prevent major cognitive injuries using the beneficial effects of antioxidants.

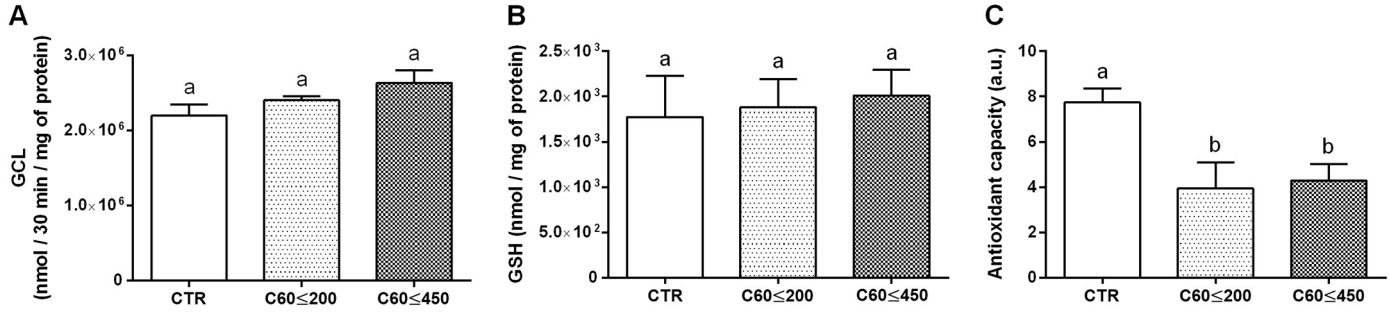

Fig. 5. Effects of the intrahippocampal infusion of C60 suspensions with different sized particles in the antioxidant defenses. No differences in glutamate cysteine ligase (GCL) and glutathione (GSH) levels were observed among the treatments [($F(2, 11) = 2.7362$ and $F(2, 11) = 0.1165$; subfigures A and B, respectively)], but the hippocampus of animals treated with any suspension of C60 showed a higher antioxidant capacity against peroxyl radicals [($F(2, 11) = 5.0250$] (C). Different letters indicate significant differences ($p < 0.05$) between the treatments (n = 4–5 per group).

Acknowledgments

Ândrea Kraemer, Gisele Eva Bruch, and Marcos Cordeiro are graduate fellows and and Juliane Ventura-Lima a post-doctoral fellow from the Brazilian agency CAPES. Gustavo Parfitt and Daiane Acosta received a graduate fellowship from the Brazilian agency CNPQ. Daniela Martí Barros (305268/2015-5) and José M. Monserrat are research fellows from CNPQ. This research study was supported by grants obtained from CNPQ577159/2008-9 and PRONEN/FAPERGS11/2037-9.

References

Amado, L.L., Garcia, M.L., Ramos, P.B., Freitas, R.F., Zafalon, B., Ferreira, J.L.R., Yunes, J.S., Monserrat, J.M., 2009. A method to measure total antioxidant capacity against peroxyl radicals in aquatic organisms: application to evaluate microcystins toxicity. Sci. Total Environ. 407, 2115–2123. http://dx.doi.org/10.1016/j.scitotenv.2008.11.038.

Andrievsky, G.V., Klochkov, V.K., Bordyuh, A.B., Dovbeshko, G.I., 2002. Comparative analysis of two aqueous-colloidal solutions of C60 fullerene with help of FTIR reflectance and UV–vis spectroscopy. Chem. Phys. Lett. 364, 8–17. http://dx.doi.org/10.1016/S0009-2614(02)01305-2.

Barros, D.M., Ramirez, M.R., Dos Reis, E.A., Izquierdo, I., 2004. Participation of hippocampal nicotinic receptors in acquisition, consolidation and retrieval of memory for one trial inhibitory avoidance in rats. Neuroscience 126, 651–656. http://dx.doi.org/10.1016/j.neuroscience.2004.03.010.

Bavithra, S., Sugantha Priya, E., Selvakumar, K., Krishnamoorthy, G., Arunakaran, J., 2015. Effect of melatonin on glutamate: BDNF signaling in the cerebral cortex of polychlorinated biphenyls (PCBs)—exposed adult male rats. Neurochem. Res. 40, 1858–1869. http://dx.doi.org/10.1007/s11064-015-1677-z.

Bekinschtein, P., Katche, C., Slipczuk, L.N., Igaz, L.M., Cammarota, M., Izquierdo, I., Medina, J.H., 2007. mTOR signaling in the hippocampus is necessary for memory formation. Neurobiol. Learn. Mem. 87, 303–307. http://dx.doi.org/10.1016/j.nlm.2006.08.007.

Bhattacharya, K., Mukherjee, S.P., Gallud, A., Burkert, S.C., Bistarelli, S., Bellucci, S., Bottini, M., Star, A., Fadeel, B., 2016. Biological interactions of carbon-based nanomaterials: from coronation to degradation. Nanomed. Nanotechnol. Biol. Med. 12, 333–351. http://dx.doi.org/10.1016/j.nano.2015.11.011.

Blickley, T.M., McClellan-Green, P., 2008. Toxicity of aqueous fullerene in adult and larval Fundulus heteroclitus. Environ. Toxicol. Chem. 27, 1964–1971.

Brausch, K.A., Anderson, T.A., Smith, P.N., Maul, J.D., 2011. The effect of fullerenes and functionalized fullerenes on Daphnia magna phototaxis and swimming behavior. Environ. Toxicol. Chem. 30, 878–884. http://dx.doi.org/10.1002/etc.442.

Chen, D., Dougherty, C.A., Zhu, K., Hong, H., 2015. Theranostic applications of carbon nanomaterials in cancer: focus on imaging and cargo delivery. J. Control. Release 210, 230–245. http://dx.doi.org/10.1016/j.jconrel.2015.04.021.

Connor, B., Dragunow, M., 1998. The role of neuronal growth factors in neurodegenerative disorders of the human brain. Brain Res. Brain Res. Rev. 27, 1–39.

Dellinger, A., Zhou, Z., Connor, J., Madhankumar, A.B., Pamujula, S., Sayes, C.M., Kepley, C.L., 2013. Application of fullerenes in nanomedicine: an update. Nanomedicine 8, 1191–1208. http://dx.doi.org/10.2217/nnm.13.99.

Ehrich, M., Van Tassell, R., Li, Y., Zhou, Z., Kepley, C.L., 2011. Fullerene antioxidants decrease organophosphate-induced acetylcholinesterase inhibition in vitro. Toxicol. in Vitro 25, 301–307.

Ferreira, J.L.R., Barros, D.M., Geracitano, L.A., Fillmann, G., Fossa, C.E., de Almeida, E.A., de Castro Prado, M., Neves, B.R.A., Pinheiro, M.V.B., Monserrat, J.M., 2012. In vitro exposure to fullerene C(60) influences redox state and lipid peroxidation in brain and gills from Cyprinus carpio (Cyprinidae). Environ. Toxicol. Chem. 31, 961–967. http://dx.doi.org/10.1002/etc.1792.

Ferreira-Cravo, M., Piedras, F.R., Moraes, T.B., Ferreira, J.L.R., de Freitas, D.P.S., Machado, M.D., Geracitano, L.A., Monserrat, J.M., 2007. Antioxidant responses and reactive oxygen species generation in different body regions of the estuarine polychaeta Laeonereis acuta (Nereididae). Chemosphere 66, 1367–1374. http://dx.doi.org/10.1016/j.chemosphere.2006.06.050.

Francis, B.M., Kim, J., Barakat, M.E., Fraenkl, S., Yücel, Y.H., Peng, S., Michalski, B., Fahnestock, M., McLaurin, J., Mount, H.T., 2012. Object recognition memory and BDNF expression are reduced in young TgCRND8 mice. Neurobiol. Aging 33, 555–563.

Gil-Bea, F.J., Solas, M., Mateos, L., Winblad, B., Ramírez, M.J., Cedazo-Mínguez, A., 2011. Cholinergic hypofunction impairs memory acquisition possibly through hippocampal Arc and BDNF downregulation. Hippocampus 21, 999–1009. http://dx.doi.org/10.1002/hipo.20812.

Goodarzi, S., Da Ros, T., Conde, J., Sefat, F., Mozafari, M., 2017. Fullerene: biomedical engineers get to revisit an old friend. Mater. Today 20 (8), 460–480.

Hersh, D.S., Wadajkar, A.S., Roberts, N., Perez, J.G., Connolly, N.P., Frenkel, V., Winkles, J.A., Woodworth, G.F., Kim, A.J., 2016. Evolving drug delivery strategies to overcome the blood brain barrier. Curr. Pharm. Des. 22, 1177–1193.

Hoo, C.M., Starostin, N., West, P., Mecartney, M.L., 2008. A comparison of atomic force microscopy (AFM) and dynamic light scattering (DLS) methods to characterize nanoparticle size distributions. J. Nanopart. Res. 10, 89–96. http://dx.doi.org/10.1007/s11051-008-9435-7.

Hotze, E.M., Labille, J., Alvarez, P., Wiesner, M.R., 2008. Mechanisms of photochemistry and reactive oxygen production by fullerene suspensions in water. Environ. Sci. Technol. 42, 4175–4180.

Hsieh, F.Y., Zhilenkov, A.V., Voronov, I.I., Khakina, E.A., Mischenko, D.V., Troshin, P.A., Hsu, S.-H., 2017. Water-soluble fullerene derivatives as brain medicine: surface chemistry determines if they are neuroprotective and antitumor. ACS Appl. Mater. Interfaces. http://dx.doi.org/10.1021/acsami.7b01077.

Injac, R., Radic, N., Govedarica, B., Perse, M., Cerar, A., Djordjevic, A., Strukelj, B., 2009. Acute doxorubicin pulmotoxicity in rats with malignant neoplasm is effectively treated with fullerenol C60(OH)24 through inhibition of oxidative stress. Pharmacol. Rep. 61, 335–342.

Johnston, H.J., Hutchison, G.R., Christensen, F.M., Aschberger, K., Stone, V., 2010. The biological mechanisms and physicochemical characteristics responsible for driving fullerene toxicity. Toxicol. Sci. 114, 162–182. http://dx.doi.org/10.1093/toxsci/kfp265.

Kamat, J.P., Devasagayam, T.P., Priyadarsini, K.I., Mohan, H., Mittal, J.P., 1998. Oxidative damage induced by the fullerene C60 on photosensitization in rat liver microsomes. Chem. Biol. Interact. 114, 145–159.

Kato, S., Kikuchi, R., Aoshima, H., Saitoh, Y., Miwa, N., 2010. Defensive effects of fullerene-C60/liposome complex against UVA-induced intracellular reactive oxygen species generation and cell death in human skin keratinocytes HaCaT, associated with intracellular uptake and extracellular excretion of fullerene-C60. J. Photochem. Photobiol. B 98, 144–151. http://dx.doi.org/10.1016/j.jphotobiol.2009.11.015.

Khalin, I., Alyautdin, R., Ismail, N.M., Haron, M.H., Kuznetsov, D., 2014. Nanoscale drug delivery systems and the blood–brain barrier. Int. J. Nanomedicine 795. http://dx.doi.org/10.2147/IJN.S52236.

Kim, M.E., Park, H.R., Gong, E.J., Choi, S.Y., Kim, H.S., Lee, J., 2011. Exposure to bisphenol A appears to impair hippocampal neurogenesis and spatial learning and memory. Food Chem. Toxicol. 49, 3383–3389. http://dx.doi.org/10.1016/j.fct.2011.09.017.

Kroto, H.W., Heath, J.R., O'Brien, S.C., Curl, R.F., Smalley, R.E., 1985. C60: Buckminsterfullerene. Nature 318, 162–163. http://dx.doi.org/10.1038/318162a0.

Larner, S.F., Wang, J., Goodman, J., Altman, M.B.O., Xin, M., Wang, K.K.W., 2017. In vitro neurotoxicity resulting from exposure of cultured neural cells to several types of nanoparticles. J. Cell Death 10. http://dx.doi.org/10.1177/1179670717694523.

Lin, A.M., Chyi, B.Y., Wang, S.D., Yu, H.-H., Kanakamma, P.P., Luh, T.-Y., Chou, C.K., Ho, L.T., 1999. Carboxyfullerene prevents iron-induced oxidative stress in rat brain. J. Neurochem. 72, 1634–1640.

Maeda-Mamiya, R., Noiri, E., Isobe, H., Nakanishi, W., Okamoto, K., Doi, K., Sugaya, T., Izumi, T., Homma, T., Nakamura, E., 2010. In vivo gene delivery by cationic tetraamino fullerene. Proc. Natl. Acad. Sci. U. S. A. 107, 5339–5344. http://dx.doi.org/10.1073/pnas.0909223107.

Markovic, Z., Trajkovic, V., 2008. Biomedical potential of the reactive oxygen species generation and quenching by fullerenes (C60). Biomaterials 29, 3561–3573. http://dx.doi.org/10.1016/j.biomaterials.2008.05.005.

Morris, R., 1984. Developments of a water-maze procedure for studying spatial learning in the rat. J. Neurosci. Methods 11, 47–60.

Oakes, K.D., Van Der Kraak, G.J., 2003. Utility of the TBARS assay in detecting oxidative stress in white sucker (Catostomus commersoni) populations exposed to pulp mill effluent. Aquat. Toxicol. (Amst. Neth.) 63, 447–463.

Oberdörster, E., 2004. Manufactured nanomaterials (fullerenes, C60) induce oxidative stress in the brain of juvenile largemouth bass. Environ. Health Perspect. 112, 1058–1062.

Paxinos, G., Watson, C., 2007. The Rat Brain in Stereotaxic Coordinates, 6th ed. Academic Press/Elsevier, Amsterdam; Boston.

Petzold, A., Psotta, L., Brigadski, T., Endres, T., Lessmann, V., 2015. Chronic BDNF deficiency leads to an age-dependent impairment in spatial learning. Neurobiol. Learn. Mem. 120, 52–60.

Pi, J., Diwan, B.A., Sun, Y., Liu, J., Qu, W., He, Y., Styblo, M., Waalkes, M.P., 2008. Arsenic-induced malignant transformation of human keratinocytes: involvement of Nrf2. Free Radic. Biol. Med. 45, 651–658. http://dx.doi.org/10.1016/j.freeradbiomed.2008.05.020.

Pilly, P.K., Grossberg, S., 2012. How do spatial learning and memory occur in the brain? Coordinated learning of entorhinal grid cells and hippocampal place cells. J. Cogn. Neurosci. 24, 1031–1054. http://dx.doi.org/10.1162/jocn_a_00200.

Pisu, M.G., Dore, R., Mostallino, M.C., Loi, M., Pibiri, F., Mameli, R., Cadeddu, R., Secci, P.P., Serra, M., 2011. Down-regulation of hippocampal BDNF and Arc associated with improvement in aversive spatial memory performance in socially isolated rats. Behav. Brain Res. 222, 73–80. http://dx.doi.org/10.1016/j.bbr.2011.03.021.

Radiske, A., Rossato, J.I., Gonzalez, M.C., Köhler, C.A., Bevilaqua, L.R., Cammarota, M., 2017. BDNF controls object recognition memory reconsolidation. Neurobiol. Learn. Mem. 142, 79–84.

Sayes, C.M., Fortner, J.D., Guo, W., Lyon, D., Boyd, A.M., Ausman, K.D., Tao, Y.J., Sitharaman, B., Wilson, L.J., Hughes, J.B., West, J.L., Colvin, V.L., 2004. The differential cytotoxicity of water-soluble fullerenes. Nano Lett. 4, 1881–1887. http://dx.doi.org/10.1021/nl0489586.

Usenko, C.Y., Harper, S.L., Tanguay, R.L., 2008. Fullerene C60 exposure elicits an oxidative stress response in embryonic zebrafish. Toxicol. Appl. Pharmacol. 229, 44–55. http://dx.doi.org/10.1016/j.taap.2007.12.030.

Wang, L., Pal, A.K., Isaacs, J.A., Bello, D., Carrier, R.L., 2014. Nanomaterial induction of oxidative stress in lung epithelial cells and macrophages. J. Nanopart. Res. 16, 2591.

White, C.C., Viernes, H., Krejsa, C.M., Botta, D., Kavanagh, T.J., 2003. Fluorescence-based microtiter plate assay for glutamate-cysteine ligase activity. Anal. Biochem. 318, 175–180.

Winston, G.W., Regoli, F., Dugas, A.J., Fong, J.H., Blanchard, K.A., 1998. A rapid gas chromatographic assay for determining oxyradical scavenging capacity of antioxidants and biological fluids. Free Radic. Biol. Med. 24, 480–493.

Xiao, L., Takada, H., Maeda, K., Haramoto, M., Miwa, N., 2005. Antioxidant effects of

water-soluble fullerene derivatives against ultraviolet ray or peroxylipid through their action of scavenging the reactive oxygen species in human skin keratinocytes. Biomed. Pharmacother. 59, 351–358. http://dx.doi.org/10.1016/j.biopha.2005.02.004.

Yamada, T., Nakaoka, R., Sawada, R., Matsuoka, A., Tsuchiya, T., 2010. Effects of intracerebral microinjection of hydroxylated-[60] fullerene on brain monoamine concentrations and locomotor behavior in rats. J. Nanosci. Nanotechnol. 10, 604–611.

Zhu, X., Zhu, L., Lang, Y., Chen, Y., 2008. Oxidative stress and growth inhibition in the freshwater fish Carassius auratus induced by chronic exposure to sublethal fullerene aggregates. Environ. Toxicol. Chem. 27, 1979–1985.